Fuel 139 (2015) 374–382

Contents lists available at ScienceDirect

Fuel

journal homepage: www.elsevier.com/locate/fuel

A novel soluble nano-catalysts in diesel–biodiesel fuel blends to improve diesel engines performance and reduce exhaust emissions

Mehrdad Mirzajanzadeh [a], Meisam Tabatabaei [b,c,*], Mehdi Ardjmand [a,b,*], Alimorad Rashidi [b,d], Barat Ghobadian [b,e], Mohammad Barkhi [b,f], Mohammad Pazouki [g]

[a] Department of Chemical Engineering, Science & Research Branch, Islamic Azad University, Tehran, Iran
[b] Biofuel Research Team (BRTeam), Karaj, Iran
[c] Microbial Biotechnology and Biosafety Department, Agricultural Biotechnology Institute of Iran (ABRII), 31535-1897 Karaj, Iran
[d] Nanotechnology Research Center, Research Institute of Petroleum Industry (RIPI), Tehran, Iran
[e] Department of Mechanics Engineering of Agricultural Machinery, Tarbiat Modares University, Tehran, Iran
[f] Geological Research Center of Iran (GRCIR), Karaj, Iran
[g] Department of Energy, Materials and Energy Research Center, MeshkinDasht, Karaj, Iran

HIGHLIGHTS

- Reporting a novel soluble (homogenous) amide-functionalized MWCNTs-CeO_2 catalyst.
- Significant improvements in combustion of B20$_{(90\ ppm)}$ compared to neat B20.
- NO_x, CO, HC and soot were reduced by up to 18.9%, 38.8%, 71.4% and 26.3%, respectively.
- Increased power and torque by up to 7.81% and 4.91%, respectively.
- Decreased fuel consumption by 4.50%.

GRAPHICAL ABSTRACT

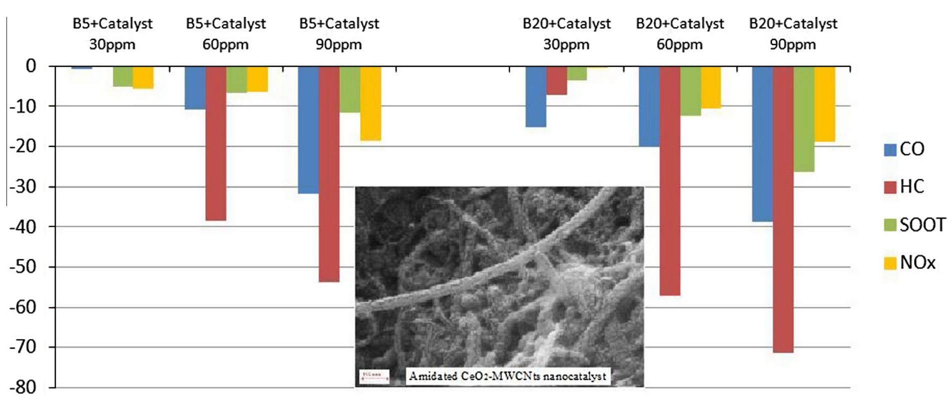

ARTICLE INFO

Article history:
Received 3 April 2014
Received in revised form 24 August 2014
Accepted 3 September 2014
Available online 19 September 2014

Keywords:
Hybrid nano-catalyst
Diesel
Biodiesel

ABSTRACT

This study was aimed at synthesizing a novel soluble hybrid nanocatalyst to decrease emissions i.e., nitrogen oxide compounds (NO_x), carbon monoxide (CO), unburned hydrocarbons (HC) and soot, of a DI engine fueled with diesel–biodiesel blends. Moreover, enhancement of performance parameters i.e. power, torque and fuel consumption was also simultaneously targeted. The hybrid nanocatalyst containing cerium oxide on amide-functionalized multiwall carbon nanotubes (MWCNT) was investigated using two types of diesel–biodiesel blends (B5 and B20) at three concentrations (30, 60 and 90 ppm). The results obtained revealed that high surface area of the soluble nano-sized catalyst particles and their proper distribution along with catalytic oxidation reaction resulted in significant overall improvements in the combustion reaction specially in B20 containing 90 ppm of the catalyst B20$_{(90\ ppm)}$. More specifically, all pollutants i.e., NO_x, CO, HC and soot were reduced by up to 18.9%, 38.8%, 71.4% and 26.3%,

Abbreviations: bmep, brake mean effective pressure; bsfc, brake specific fuel consumption; bte, brake thermal efficiency; CCCFP, close cup flash point; CNT, carbon nanotube; CO, carbon monoxide; CO_2, carbon dioxide; CVD, chemical vapor deposition; DI engine, direct injection engine; HC, unburned hydrocarbons; MWCNT, multi wall carbon nanotube; NO_x, nitrogen oxides; SEM, scanning electron microscope; SO_x, sulphur oxides.

* Corresponding authors at: Biofuel Research team (BRTeam), Agricultural Biotechnology Institute of Iran (ABRII), 31535-1897 Karaj, Iran. Tel.: +98 26 32703536; fax: +98 26 32701067 (M. Tabatabaei). Department of Chemical engineering, Science and Research Branch, Islamic Azad University, 1477893855 Tehran, Iran. Tel.: +98 21 47911; fax: +98 21 44867141 (M. Ardjmand).

E-mail addresses: meisam_tab@yahoo.com (M. Tabatabaei), m_arjmand@azad.ac.ir (M. Ardjmand).

http://dx.doi.org/10.1016/j.fuel.2014.09.008
0016-2361/

Emissions
Engine performance

respectively, in $B20_{(90\ ppm)}$ compared to neat B20. The innovated fuel blend also increased engine performance parameters i.e., power and torque by up to 7.81%, 4.91%, respectively, and decreased fuel consumption by 4.50%.

Nomenclature

B5	biodiesel 5% + diesel 95%
B20	biodiesel 20% + diesel 80%
B100	neat biodiesel
$B5_{(30\ ppm)}$	B5 + 30 ppm nanocatalyst
$B5_{(60\ ppm)}$	B5 + 60 ppm nanocatalyst
$B5_{(90\ ppm)}$	B5 + 90 ppm nanocatalyst
$B20_{(30\ ppm)}$	B20 + 30 ppm nanocatalyst
$B20_{(60\ ppm)}$	B20 + 60 ppm nanocatalyst
$B20_{(90\ ppm)}$	B20 + 90 ppm nanocatalyst
Ce	cerium
Ir	iridium
Pd	palladium
Pt	platinum
Rh	rhodium

1. Introduction

It is known almost to every resident of the planet Erath that fossil fuel resources are depleting day by day and hence, there is a need to search for alternative fuels to fulfill the growing energy demands of the world [1]. More importantly, the environmental crises caused by vast combustion of fossil fuels have also led researchers towards finding strategies to address the critically-worrying level of air pollution and its potentially tragic consequences e.g., climate change [2]. Among the various alternative fuels, biofuels (in particular liquid biofuels e.g., bioethanol, biobuthanol and biodiesel), have received a great deal of attention as the most desirable fuel extenders for the transportation sector [1–6]. This is ascribed to the fact that these energy carriers are capable of powering machines on their own while their harmful emissions such as SO_x, HC, and CO are considerably less in comparison with those of the fossil fuels [7–10].

Biodiesel (methyl or ethyl esters of fatty acids), possesses characteristics similar to those of diesel while the biggest difference is its oxygen content resulting in a more complete combustion and consequently higher energy generation (higher cetane number) [11,12]. Nevertheless, the overall energy obtained through biodiesel combustion is less than that of diesel fuel [13]. It should also be noted that a number of reports argue that unwanted increases in NO_x emission were caused by biodiesel inclusion [14]. In fact the major drawback associated with the application of biodiesel fuel blends is increased NO_x emission in comparison with petro-diesel [15]. Therefore, a number of attempts have been made to boost the performance of biodiesel-fed engines while maintaining emissions as low as possible. Among such attempts has been the application of heterogeneous or homogenous catalysts. Boutonnet et al. [16] first studied the monodispersed metal particles i.e. Pt, Pd, Rh and Ir in form of microemulsion. They showed that it is possible to prepare monodispersed suspensions of metals in organic solvents by dissolving them in ionic form in the interior of reversed micelles in micro emulsions followed by reduction with an appropriate reducing agent. Their findings paved the path for the other researchers to investigate other metal additives for promoting fuel properties and engine performance and reducing pollutants [14–23]. For instance, Basha and Anand [20] carried out experimental investigations to study the effects of alumina nanoparticle blended into an emulsion fuel (5% water, 93% jatropha biodiesel, 2% surfactants) on combustion characteristics of a diesel engine. In fact, they looked into ultrasound-assisted inclusion of alumina nanoparticles at two different rates of 25 and 50 ppm. The results revealed a considerable enhancement of 29% in brake thermal efficiency (bte) compared to the neat biodiesel at full load. Later in 2013, Basha and Anand [21] in a different investigation evaluated the potential application of nano-alumina particles and carbon nanotubes (CNT) at two concentrations of 25 and 50 ppm in a diesel engine fed with different jatropha biodiesel–diesel blends in order to improve engine performance and reduce emissions. They observed maximum bte of 28.9% at full load for jatropha biodiesel supplemented with 25 ppm nano-alumina and 25 ppm CNT(JBD25A25CNT), whereas this value was measured at 27.1%, 27.9%, and 24.9% for jatropha biodiesel supplemented with 50 ppm CNT(JBD50CNT), jatropha biodiesel supplemented with 50 ppm alumina(JBD50A), and neat jatropha biodiesel(JBD) at the full load, respectively. Moreover, the NO_x and smoke emissions were reduced for nanoparticles-containing jatropha biodiesel fuels compared to those of the neat jatropha biodiesel fuel. The magnitude of smoke opacity observed was 57% for JBD25A25CNT, whereas it stood at 60%, 58% and 67% for JBD50CNT, JBD50A and JBD at full load, respectively. The magnitude of NO_x emissions observed was 1282 ppm for JBD, whereas it was measured at 1015, 1001, and 985 ppm for JBD50A, JBD50CNT, and JBD25A25CNT at the full load, respectively.

Li [22] also attempted to scrutinize the combustion behavior of nano-aluminum (n-Al) (1%, 3%, 5%, 7%, and 10% v/v), and nano-aluminum oxide (n-Al2O3)(0.5%, 1%, 3%, and 5%, v/v) particles, stably suspended in bioethanol. He studied the heat of combustion using a modified static bomb calorimeter system and N—Al and n-Al2O3 particles of 50 nm and 36 nm diameters, respectively, were utilized. The results obtained indicated that the amount of heat released from ethanol combustion increased almost linearly with n-Al concentration. N—Al volume fractions of 1% and 3% did not show enhancement in the average volumetric heat of combustion, but higher volume fractions of 5%, 7%, and 10% increased the volumetric heat of combustion by 5.82%, 8.65%, and 15.31%, respectively. He concluded that the n-Al_2O_3 and heavily passivated n-Al additives did not participate in combustion reactively. In a different study, Tewari et al. reported combustion characteristics of multi walled carbon nanotubes (MWCNTs) blended into biodiesel fuel. They used a mechanical homogenizer (ultrasonicator) to disperse the catalyst at two different levels of 25 and 50 ppm. The results at a constant speed of 1500 rpm revealed a considerable enhancement in the brake thermal efficiency and a substantial reduction in the emission of harmful pollutants due to the incorporation of MWCNTs in the biodiesel fuel [23].

On the other hand, catalyst activity strongly depends on the size or in another word; smaller particles possess higher catalytic activity [24–26]. Also, nano-scale particles spread more uniformly within the liquid (such as liquid fuels) and are more stable than those out of this range. so, the nanocatalysts are much more effective [27–29]. These established the basis for a number of studies on the application of metal nanoparticles at nanoscale.

A number of experimental studies [30,31] were also conducted on the effect of cerium oxide nano-particles (nanocera) as an additive to various fuel mixtures in direct injection engines. The results showed that the cerium oxide nano-particles could be used as additive to diesel fuel and diesel–biodiesel–ethanol mixture to achieve a completer combustion and significant reductions of exhaust emissions. In a more recent study, Sajith and Sobhan [30] reported the impact of nanocera on major physicochemical properties of B100 as well as engine performance and emissions parameters. Their findings revealed an increase in fuel's flash point and viscosity owing to the inclusion of the cerium oxide nanoparticles. They also argued that the nanocatalyst at concentrations ranging from 40 to 80 ppm resulted in an average reduction of hydrocarbon emissions by 25% to 40% and at its highest inclusion rate of 80 ppm led to 30% reduction in NO_x. Later in 2009, Arul Mozhi Selvan et al. [31] added nanocera to neat diesel and diesel–biodiesel–ethanol blends, and reported that cerium oxide nanoparticles led to decreases in CO, NO and smoke. They also concluded that the addition of cerium oxide nanoparticles decreased the ignition delay. In better words, the addition of nanocera accelerated earlier initiation of combustion and lowered the heat release rate when comparing with diesel–biodiesel–ethanol blend.

In 2008, Boutonnet et al. [32] reviewed the works done in this field. They highlighted that the use of heterogeneous solid catalysts would not be practical, as continuously exposing a supplied catalyst to the extremely high temperatures encountered in the combustion environment would quickly deactivate the catalyst. On such basis, the other way to introduce catalysts as investigated in the present study, would be to dissolve them in fuel so that they could be added on a continuous basis. More importantly, soluble catalyst particles do not settle out during the injection stage and neither interfere with the engine operation [33–35].

Therefore, the aim of this study was to investigate the effect of a novel soluble catalyst on performance and emission characteristics of a DI diesel engine fueled with biodiesel-blended diesel fuel. The catalyst i.e. cerium oxide nano-particles on amide-functionalized multiwall carbon nanotubes (MWCNT-amide), was added to two fuel blends of diesel–biodiesel (B5 and B20) at 3 different concentrations (30, 60 and 90 ppm) ($B5_{30\ ppm,60\ ppm,90\ ppm}$ and $B20_{30\ ppm,60\ ppm,90\ ppm}$, respectively) and engine performance parameters such as power, torque and bsfc as well as exhaust emissions i.e., CO, NO_x, HC and soot were investigated.

2. Materials and methods

2.1. Materials

MWCNTs prepared by chemical vapor deposition (CVD) method over Co—Mo/MgO catalyst was obtained from the Institute of Petroleum Industry (R.I.P.I., Iran) with the purity of 90–95%. The average diameter of the nanotubes varied from 7 to 20 nm with their length ranging from 5 to 15 μm. Chemicals including thionyl chloride (99.5%) and ethanol (99%) were purchased from Acros Organics Co. (USA) and Merck Co. (Germany), respectively. Also, nano-cerium oxide (CeO_2) with <25 nm particle size, KOH (99%), methanol (99%), N,N-Dimethylformamide (DMF, 99%), octadecylamine (98%) and anhydrous tetrahydrofuran (THF, 99%) were provided by Aldrich Chemical Co. (USA). Biodiesel was produced from waste cooking oil and neat diesel fuel was provided by Tabriz oil refinery (Iran).

2.2. Equipment and procedures

2.2.1. Fuel blends preparation and analyses

Biodiesel was produced from pretreated waste cooking oil through KOH-catalyzed transesterification reaction (oil/methanol ratio: 6/1, 60 °C, 1 wt.% KOH, 1 h). More specifically, the acid value of the oil was measured at 16 mg KOH/g corresponding to 8% FFA which was above the 1% limit required for achieving an efficient transesterification reaction using alkaline catalysts. Therefore, a pretreatment process was carried out with the methanol-to-oil ratio of 0.3 (v/v) in the presence of 1% H_2SO_4 (v/v) as an acid catalyst for 1 h at 60 °C. After the reaction, the mixture was allowed to settle for 1 h and the methanol–water fraction separated at the top was removed. The acid value of the bottom phase was determined and if the value was measured at above 2 mg KOH/g corresponding to 1% FFA, the pretreatment step was repeated before proceeding to the transesterification reaction. Biodiesel–diesel blends (B5, B20 and B100) were then prepared. Flash point of the studied fuel blends were measured by a continuously close cup flash point (CCCFP) tester using a Grabner FLPH Miniflash Tester (Grabner, Austria). Dynamic and kinematic viscosities and density were determined by Stabinger Viscometer, Anton Paar, SVM3000 model (Anton Paar Co., Austria). Karl Fischer setup, metrohm, 794 Basic Titrino model was used for water and sediment content measurements. The composition of the biodiesel produced by transesterification of waste cooking oil was determined using Gas Chromatography (GC, Claus 580 GC model, Perkin Elmer Co., USA) and the methyl ester capillary column used for GC analysis was purchased from Varian Co. (model: CP 9080) with 30 m length and 0.32 mm internal diameter.

2.2.2. Nano-catalysts synthesis and characterization

Nano cerium oxide was hybridized with MWCNTs using the solvent-aided method [36] and was then calcinated at 460 °C for 3 h at the 5 °C/min rate. Five grams of the hybridized CeO_2-MWNTs were carboxyl-functionalized by first ozonation at room temperature and atmospheric condition for 4 h. Then, the ozonated CeO_2-MWNTs was cleaved by using hydrogen peroxide. More specifically, the ozonized CeO_2-MWNTs were refluxed for 1 h at 60 °C in 36% H_2O_2 aqueous solution and then the mixture was stirred at room temperature for 20 h. Subsequently, the solution was passed through a 0.2 mm polycarbonate membrane, washed with methanol, and oven-dried at 100 °C. The CeO_2-MWNTs-COOH was then stirred and refluxed in a mixture of 800 ml thionyl chloride ($SOCl_2$) and 40 ml dimethylformamide (DMF) at 70 °C for 24 h. After acylchlorination, the hybridized nanocatalyst was washed with anhydrous tetrahydrofuran (THF) for five times and then dried at 40 °C for 30 min. The acyl-chlorinated nanocatalyst was then added to 25 g of octadecylamine (oda). This mixture was sonicated using an ultrasound bath at 60 °C in 40 GHz for 2 h, and then refluxed for 2 days. After cooling to room temperature, the amidated product was washed with ethanol to remove excess amine. Finally, the nanocatalyst containing CeO_2 and amides functional groups was dried at 70 °C overnight [37–42].

The raw and hybridized MWCNTs were analyzed using a ZEISS scanning electron microscope (SEM) (Germany) at 20.0 kV. A NexION®300 ICP-MS (Perkin Elmer, USA) was used to determine the mole fraction of the CeO_2 embedded on MWCNTs prior to functionalization. FTIR spectra were obtained using an FTIR Ray Leigh WQF-510A and were employed to examine the chemical composition of the final product or in another word the nanocatalyst used; amidated CeO_2-MWCNTs.

2.2.3. Engine performance and emissions: Experimental

The nanocatalyst was added to the biodiesel blends (B5 and B20) at 3 concentrations at 30, 60 and 90 ppm. Then, the samples were placed at an ultrasonic bath for 30 min (40 Hz) in order to obtain well-dispersed and highly-stable fuel blends. Performance characteristics of the investigated fuel blends were tested using a 13-mode steady-state test with an upgraded version of OM355 EU2 engine at IDEM Co. (Tabriz, Iran), under German-Mercedes Benz license with EUROII emission certification awarded by T□V NORD (Germany). Table 1 tabulates the technical specification of the engine. The experimental setup was coupled to a dynamometer and a computerized data acquisition system was used to collect, store and analyze the data. The load applied on the engine was measured by a load cell connected to the dynamometer. A burette optical sensor and an air-flow sensor were used to compute fuel flow rate and inlet air flow rate, respectively. Two thermocouples were applied to measure inlet air and exhaust gas temperatures.

Performance characteristics of the investigated fuels were conducted at 1000, 1200, 1400, 1500, 1600, 1800, 2000 and 2200 rpm at full load and the maximum torque was obtained at 1500 rpm. Therefore, the engine performance parameters including power, torque and bsfc were reported in the manuscript at the speed of 1500 rpm. Combustion experiments to characterize emissions were tested using a 13-mode steady-state test. The test includes a sequence of 13 steady-state modes, which simulates vehicle movement under road conditions. The emissions are averaged over the entire cycle using a set of weighting factors and are expressed in g/kW h. The 13-mode test parameters for the diesel cycle and the specific fuel flow rates for all the combustion experiments conducted in this study are tabulated in Table 2.

The values obtained were corrected based on the existing ambient pressure (864 mbar), humidity (40%) and temperature (26 °C) during the experiments.

Engine emissions were determined using an AVL Dicom4000-class1 exhaust gas analyzer. CO and CO_2 were measured using a non-dispersive infrared detector (NDIR) while a chemical luminescence detector (CLD) was used for NO_x measurements. Smoke was determined using an AVL 415S smoke meter (Fig. 1).

Table 1
Technical specification of the engine OM355 EU2.

Specification	Explanations
Type	Heavy duty D.I. diesel engine
No. of cylinders	6, Vertical-inline
Max. power	240 hp @ 2200 rpm
Max. torque	820 Nm @ 1400 rpm
Compression ratio	16.82
Cylinder bore	128 mm
Stroke	150 mm
Engine dimensions	1335 * 685 * 1085(l * w * h) mm
Total engine weight	880 kg
Total piston displacement	11.580 l
Min. fuel consumption	203.8 g/kW h @ 1000 rpm
Rotation	C.C.W
Cooling	Water cooled
Compression ratio	16.1:1
No. of nozzles/injector	4
Nozzle opening pressure	195 bar
IVC	61 °C A after BDC
EVO	60 °C A before BDC
Emission standard	EURO2

Table 2
The 13-mode test parameters for the diesel cycle and the specific fuel flow rates for all the combustion experiments conducted in the present study.

Mode	Nominal speed (%)	Load (%)	Weighting factor	Specific fuel flow rate (kg/h)
1	Idle	–	0.410/2	1.2
2	40	20	0.037	6.3
3	40	40	0.027	7.8
4	Idle	–	0.410/2	13.5
5	60	20	0.029	19.9
6	60	40	0.064	26.8
7	80	40	0.041	1.1
8	80	60	0.032	38.3
9	60	60	0.077	29.6
10	60	80	0.055	21.3
11	60	95	0.049	14.9
12	80	80	0.037	11.3
13	60	5	0.142	1.1

2.2.4. Engine performance and emissions: Theoretical

2.2.4.1. Power. Power is defined as force available for the crankshaft and is obtained as follows [43]:

$$P_b\ (\text{kW}) = \frac{2\pi \cdot \omega \cdot \tau}{1000} \quad (1)$$

where τ is brake torque (N m) and ω is crankshaft rotational speed (rev/s), In practice, power is measured by using a dynamometer as follows:

$$\text{Power} = \frac{\text{dynamometer read number} \times \text{engine speed}}{\text{dynamometer constant number}} \quad (2)$$

2.2.4.2. Torque. Torque is a good indicator of the engine ability to rotate. Torque is defined as force that acts at a distance to create momentum as is calculated using the following equation [43]:

$$2\pi\tau = \frac{\text{bmep} \cdot V_d}{n_r} \quad (3)$$

where τ is torque, n_r is the number of crank revolutions for one complete cycle, V_d is displacement volume of cylinders and bmep is brake mean effective pressure (Pa).

2.2.4.3. Brake specific fuel consumption (bsfc). The brake specific fuel consumption (bsfc) is a yardstick of complete consumption in the combustion chamber and economically is a good yardstick showing fuel consumption by a vehicle and the produced power at a given time. In fact, fuel consumption would be greater at conditions far from ideal combustion conditions. The bsfc value is calculated as follows [43,44]:

$$bsfc\ (\text{g/kW h}) = \frac{\dot{m}_f}{p_b} \times 10^3 \quad (4)$$

where, $\dot{m}_f$ (kg/h) is mass rate of input fuel to the engine.

3. Results and discussion

3.1. Nanocatalyst (CeO_2-MWCNTs) synthesis and characterization

ICP mass results revealed that the synthesized CeO_2-MWCNTs contained 46% Ce and the FTIR spectra confirmed the successful fabrication of the nanocatalyst (Fig. 2). More specifically, the peak observed at 3374 cm^{-1} could be assigned to the stretching vibration of the hydrogen-bonded OH groups. The peak at 1600 cm^{-1} corresponds to C=C of the MWCNTs. Moreover, the weak peaks at less than 1000 cm^{-1} were assigned to the Ce—O—C vibrational

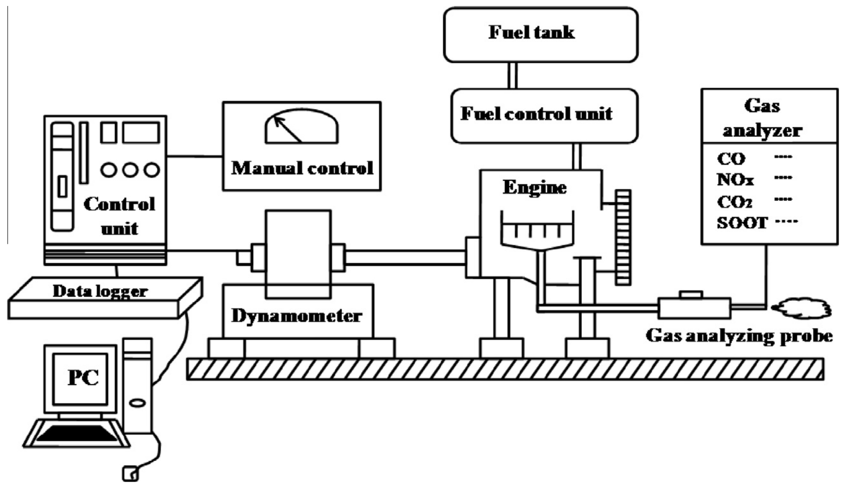

Fig. 1. Schematic figure of the diesel test engine setup.

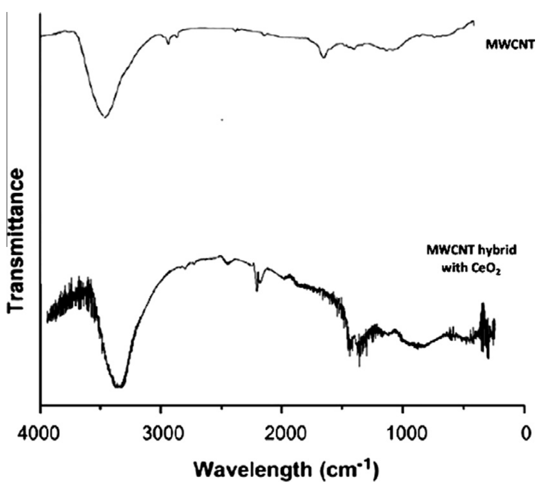

Fig. 2. The FTIR spectra of the MWCNTs and the amidated CeO_2-MWCNts.

stretch. The FTIR spectrum also shows a peak at 445 cm^{-1} representing the Ce—O stretching bond.

Scanning electron microscopy (SEM) images obtained revealed the structures of the MWCNTs prior to hybridization/amidation processes (Fig. 3a) and the amidated CeO_2-MWCNts (Fig. 3b). Fig. 3 shows that the synthesized MWCNTs possessed a long and straight structure with an average external diameter of 7–20 nm. It also could be well comprehended that the microstructure of the NWCNTs was not destroyed by the amidation reaction. The CeO_2 hybridization led to increase the diameter of the tubes to 40–50 nm.

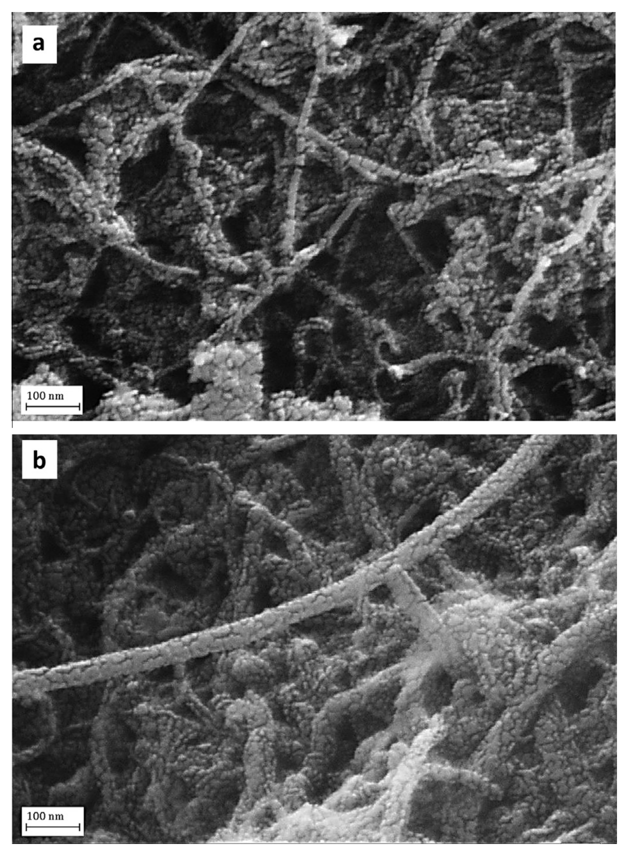

Fig. 3. Scanning electron microscopy (SEM) micrographs of the MWCNTs, (a) prior to hybridization/amidation processes and (b), the amidated CeO_2-MWCNts.

3.2. Fuel characterization

The fatty acid methyl ester (FAME) profile of the produced biodiesel from waste cooking oil as well as the FAME profile of the main biodiesel feedstocks [45] are presented in Table 3. Table 4 tabulates the physicochemical properties of the produced biodiesel and fuel blends.

3.3. Engine performance characteristics

3.3.1. Performance parameters

Fig. 4 presents the power obtained using different fuel blends (B5 and B20) with 3 concentrations of the catalyst at maximum torque of 1500 rpm at full load. The results obtained revealed that the produced power was directly proportional to the amount of the nanocatalyst applied and that the relation was approximately linear. More specifically, addition of the nanocatalyst at 30, 60 and 90 ppm resulted in 0.58%, 1.79% and 3.52% for B5 and 2.28%, 5.72% and 7.81% increase in power production for B20, respectively, in comparison to their nanocatalyst free counterparts.

Fig. 5 shows the results of maximum torque for different fuel blends i.e., B5 and B20 created at 1500rmp at full load and the increases achieved through the inclusion of the nanocatalyst at

Table 3
Fatty acid methyl ester (FAME) profile (wt.%) of common biodiesel feedstocks [45] and the biodiesel produced in this study.

	Fatty acid composition	Soybean	Cottonseed	Palm	Lard	Tallow	Coconut	Produced biodiesel
Saturated	Lauric (C12:0)	0.1	0.1	0.1	0.1	0.1	46.5	n/a
	Myristic (C14:0)	0.1	0.7	1.0	1.4	0.8	19.2	n/a
	Palmitic (C16:0)	0.2	20.1	42.8	23.6	23.3	9.8	20.18
	Stearic (C18:0)	3.7	2.6	4.5	14.2	19.4	3.0	3.44
	Arachidic (C20:0)	n/a	n/a	n/a	n/a	n/a	n/a	0.31
Total saturated		4.1	23.5	48.4	39.3	43.6	78.5	23.93
Unsaturated	Oleic(t) (C18:1t)	22.8	19.2	40.5	44.2	42.4	6.9	41.39
	Linoleic (C18:2)	53.7	55.2	10.1	10.7	10.7	2.2	31.42
	Linolenic (C18:3)	8.6	0.6	0.2	0.4	0.4	0	0.40
	Oleic(c) (C18:1c)	n/a	n/a	n/a	n/a	n/a	n/a	2.27
	Gadoleic (C20:1)	n/a	n/a	n/a	n/a	n/a	n/a	n/a
Total unsaturated		85.1	75	50.8	55.3	53.5	9.1	75.48
Total FAME		89.2	98.5	99.2	94.6	97.1	87.6	99.41

Table 4
Physicochemical properties of the produced biodiesel and fuel blends.

Property	Neat biodiesel (B100)	B5	B20	Limits according to ASTM D6751 (for neat biodiesel)	Units
Density (40 °C)	0.8692	0.8267	0.8344	0.86–0.90	g/cm^3
Viscosity (40 °C)	5.5410	3.3612	3.7158	1.9–6.0	mm^2/s
Flash point	171.1	68.3	71.3	>130	°C
Water and sediment	0.04	–	–	<0.05	vol.%
Oxidation stability at 110 °C	5.5	–	–	>6.0	h
Iodine value	109	–	–	<120	g iodine/100 g

different rates i.e. 30, 60 and 90 ppm. Since the produced power is directly proportional to the torque, the same trend as of power was observed for the produced torque as well. More precisely, addition of the nanocatalyst to the fuel blends (B5 and B20) at 30, 60 and 90 ppm concentrations let to 1.17%, 1.87% and 3.51% increase in the produced torque for B5 and 2.62%, 2.82% and 4.91% increase in the produced torque for B20, respectively, in comparison to their nanocatalyst-free counterparts.

The brake specific fuel consumption (bsfc) is a yardstick of complete consumption in the combustion chamber and economically is a good yardstick showing fuel consumption by a vehicle and the produced power at a given time. In fact, fuel consumption would be greater at conditions far from ideal combustion conditions. Fig. 6 presents the results of bsfc for different fuel blends. When compared to the nanocatalyst-free B5 and B20, the inclusion of the nanocatalyst at 30, 60 and 90 ppm caused 0.42%, 0.84% and 3.09% decrease in bsfc for B5 and 0.34%, 1.49% and 4.51% decrease in bsfc for B20, respectively.

The overall improving effects of the innovated nanocatalyst on engine performance parameters i.e., power, torque and bsfc could be attributed to the fact that the nano particles of cerium oxide as a catalyst provide oxygen molecules in a chain reaction causing complete combustion of unburned hydrocarbons and carbon monoxide [29,46]. The complete combustion of the fuel in the cylinder will be translated into the generation of more energy. Moreover, cerium oxide has a significant role in the combustion of residual carbon and preventing the precipitation of non-polar components on the cylinder walls. The nano-catalyst in the fuel produces millions of nano-clusters which then explode in order to disintegrate and to decompose the deposits and to prevent their re-formation [46]. Therefore, cerium oxide prevents the formation of carbon and iron deposits as well as their other derivatives. As a result, this phenomenon leads to decreased friction on the mentioned moving parts of the engine and consequently decreases fuel consumption and increase power and torque [29,46].

Moreover, by comparing the impact of the nanocatalyst on the performance characteristics of B5 and B20, it could be

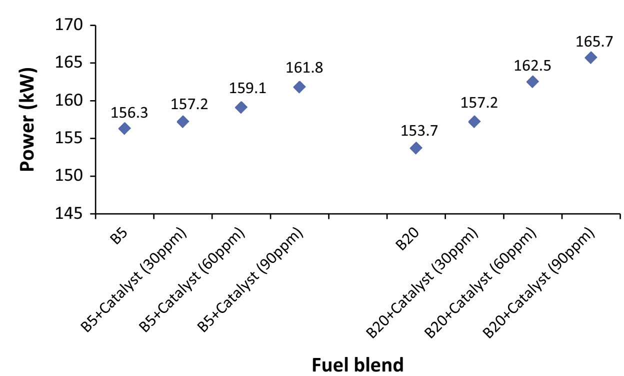

Fig. 4. Results of maximum power generated by different fuel blends (B5 and B20) containing CeO_2-MWCNTs nanocatalyst at the speed of 1500 rpm and full load.

comprehended that a kind of synergic effect existed by increasing the level of biodiesel from 5% to 20%. This could be ascribed to the higher level of oxygen provided into the combustion chamber.

3.3.2. Engine emission characteristics

Generally engine emissions are divided into two categories: Emissions produced as results of high temperature of flame and combustion chamber like NO_x and emissions produced resulting from incomplete combustion of fuel and lower flame temperature like HC and CO_2. Simultaneous control of the pollutants is difficult since different pollutants form at different temperatures [29]. Carbon monoxide is produced as a result of incomplete combustion of air–fuel mixture, low combustion cycle time in the engine or lower temperature of the combustion chamber [29]. On the other hand, incomplete combustion of fuel would lead to the emission of the unburned hydrocarbons in the exhaust stream. It is worth quoting that the profile and the concentration of these unburned hydrocarbon compounds in the exhaust effluent are dependent on both engine operating conditions and design. For instance, soot

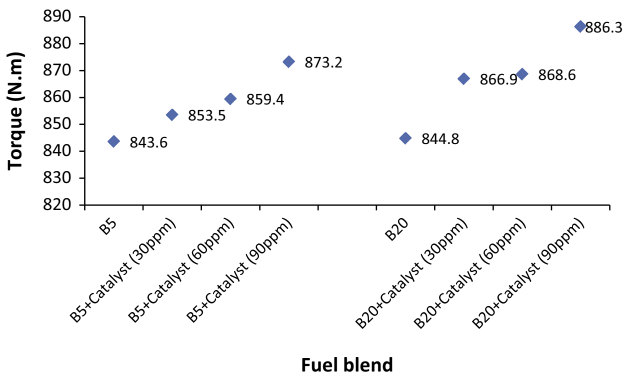

Fig. 5. Results of maximum torque by different fuel blends (B5 and B20) containing CeO_2-MWCNTs nanocatalyst at the speed of 1500 rmp and full load.

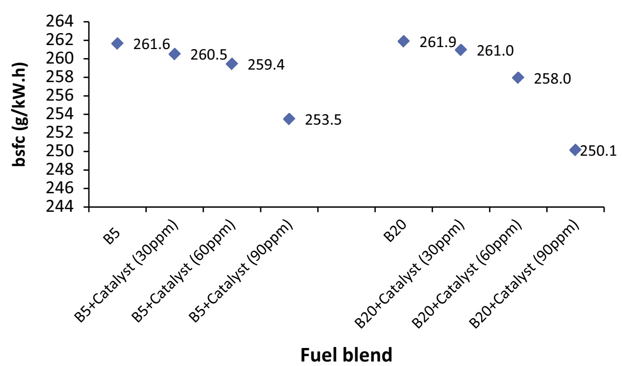

Fig. 6. Results of bsfc for different fuel blends (B5 and B20), and at different CeO_2-MWCNTs nanocatalyst inclusion rate i.e., 30, 60 and 90 ppm at the speed of 1500 rmp and full load.

is produced by incomplete combustion of the hydrocarbon fuel and is observed in the dark exhaust effluents.

Generally, by increasing the amount of available oxygen more complete combustion and consequently less emitted pollutants could be achieved. Cerium oxide is capable of preserving or liberating oxygen as shown in the following equation:

$$2CeO_2 \leftrightarrow Ce_2O_3 + \frac{1}{2}O_2 \quad (5)$$

The key to the use of ceria for catalytic purpose is the low redox potential between the Ce^{3+} and Ce^{4+} ions (1.7 V) [47] that allows the above reaction (Eq. (5)) to easily occur in exhaust gases. In fact, in the combustion chamber CeO_2 could be an oxygen scavenger or supplier via two different mechanisms. The first mechanism involves provision of the needed oxygen for oxidizing carbon monoxide or hydrocarbons and the second mechanism involves absorption of oxygen and consequent decrease of pressure in the combustion chamber. More specifically, cerium oxide may provide oxygen for the oxidation of CO or C_nH_n and through its second mechanism of action could lead to decreased production of NO_x as well [47].

Eqs. (6)–(8) present oxygen supply mechanism by cerium oxide which leads to reduced production of uncombusted hydrocarbons (HC), soot and carbon monoxide (CO), respectively.

$$(2x + y)CeO_2 + C_xH_y \leftrightarrow [(2x + y)/2]Ce_2O_3 + \frac{x}{2}CO_2 + \frac{y}{2}H_2O \quad (6)$$

$$4CeO_2 + C_{Soot} \leftrightarrow 2Ce_2O_3 + CO_2 \quad (7)$$

$$2CeO_2 + CO \rightarrow Ce_2O_3 + CO_2 \quad (8)$$

Table 5 tabulates the impact of the nanocatalyst addition at different rates on the emitted CO (g/kW h). As observed, less CO emission at all three concentration of 30, 60 and 90 ppm for both B5 and B20 in comparison with the base fuels was achieved. As mentioned earlier, this could be well explained by the first action mechanism of CeO_2 (Eq. (8))

The corresponding results for HC emission in g/kW h were shown in Table 5. The combustion of the nanocatalyst-containing fuel samples especially at the highest nanocatalyst concentration of 90 ppm resulted in the least HC emission in comparison with their catalyst free counterparts. The results for the produced soot (g/kW h) are given in Table 5, where 3.5–26.3% decrease in the produced soot was observed for nanocatalyst-containing fuel samples.

Nitrogen oxides (including NO and NO_2) are formed as a result reacting oxygen and nitrogen under high temperature conditions. In fact, NO_x production is increased by increasing the reaction temperature. The concentration of NO_x in the exhaust effluent stream is also dependent on engine design and operating conditions. When the nanocatalysts was used as additive, big drops of fuel might have burned more completely leaving less remainings in the combustion chamber. To the contrary, incomplete combustion of fuel causes more emissions and moreover leads to the formation of carbon deposit on the walls of the combustion chamber as well as on the other parts like valves. The deposits then act as insulation and increase the temperature of the combustion chamber and consequently NO_x emission; meanwhile the incomplete combustion and the deposits will contaminate motor oil. During the combustion in cylinder, the deposits become hot causing an early ignition. This in turn results in knocks in the engine which reduces the motor performance and shelf life [46].

Eq. (9) shows the mechanism of oxygen adsorption by cerium oxide which could lead to reduced NO_x production.

$$Ce_2O_3 + NO \leftrightarrow 2CeO_2 + \frac{1}{2}N_2 \quad (9)$$

On the other hand, it should be noted that complete combustion of fuel is also associated with higher temperatures leading to less deposit accumulation occurring on the internal walls of the cylinder. This in turn improves heat transfer through the cylinder walls

Table 5
The impact of the CeO_2-MWCNTs nanocatalysts inclusion in different fuel blends (B5 and B20) on CO (g/kW h), HC (g/kW h), soot (g/kW h) and NO_x (g/kW h) emissions.

Fuel blend	CO (g/kW h)	EU emission standards for CO	HC (g/kW h)	EU emission standards for HC	Soot (g/kW h)	EU emission standards for soot	NO_x	EU emission standards for NO_x
B5	6.72		0.13		0.60		5.14	
$B5_{(30\ ppm)}$	6.68	EuroII = 4	0.13	EuroII = 1.1	0.57		4.85	
$B5_{(60\ ppm)}$	5.99	EuroIII = 2	0.08	EuroIII = 0.66	0.56	EuroIII = 0.8	4.81	EuroII = 7
$B5_{(90\ ppm)}$	4.58		0.06	EuroIV and V = 0.46	0.53		4.19	EuroIII = 5
B20	6.78	EuroIV = 1.5	0.14	EuroVI = 0.13	0.57		5.25	EuroIV = 1.5
$B20_{(30\ ppm)}$	5.74	EuroV = 1.5	0.13		0.55	EuroIV and V = 0.5	5.22	EuroV = 2
$B20_{(60\ ppm)}$	5.42		0.06		0.50		4.70	
$B20_{(90\ ppm)}$	4.15		0.04		0.42		4.26	

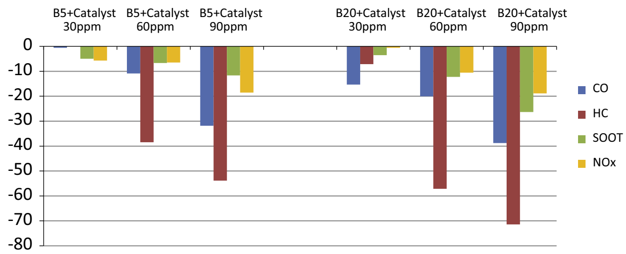

Fig. 7. Overall decrease in emissions (i.e., CO, HC, Soot and NO_x) achieved by addition of the CeO_2-MWCNTs nanocatalyst at different concentrations (30, 60 and 90 ppm) compared to catalyst-free B5 and B20.

and results in reduced NO_x production. Having mentioned the two opposite phenomena associated with complete combustion, the presence of the cera nanocatalyst as elaborated earlier provides the needed oxygen for oxidizing carbon monoxide or hydrocarbons while absorbs oxygen and consequently decreases NO_x production [47].

Table 5 also shows the produced NO_x (g/kW h) as influenced by the addition of the nanocatalyst to the fuel blends. Fig. 7 summarizes the overall effect of the nanocatalyst inclusion at 30, 60 and 90 ppm concentrations in B5 and B20 on reducing the CO, HC, soot and NO_x emissions compared to catalyst-free biodiesel blends. As clearly observed, significant decreases in all emissions proportional to the amount of the used nanocatalyst were achieved. The maximum decrease in the amounts of pollutants was observed at 90 ppm concentration of the nanocatalyst. Moreover, HC was most affected by the CeO_2-MWCNTs addition to the fuel blends.

Therefore, the overall improving effects of the innovated nanocatalyst on engine emission parameters could be attributed to the fact that the nano particles of cerium oxide as a catalyst have been reported to reduce the peak temperature in the combustion chamber resulting in decreased production of nitrogen oxides (NO_x) [46]. Moreover, they can also provide oxygen molecule in a chain reaction causing complete combustion of unburned hydrocarbons and carbon monoxide and thus reduce the amount of the pollutants. Also, the CNTs used in the innovated nanocatalyst acted as a catalyst to accelerate the combustion rate and efficiency led to reduce the amount of emissions like carbon monoxide and unburned hydrocarbons as a result of more complete combustion and increase power [48].

4. Conclusion

Soluble (homogenous) amide-functionalized MWCNTs were used as support for CeO_2 as the catalytic agent and the hybrid catalyst (CeO_2-MWCNTs) was added to the diesel–biodiesel blends (B5 and B20) at 30, 60 and 90 ppm concentrations. The unique oxygen donation/absorption properties of CeO_2 resulted in CO oxidation reaction. Moreover, CeO_2 nano particles owing to their decreasing impact on peak temperature in the combustion chamber resulted in decreased production of nitrogen oxides (NO_x). Overall, all pollutants i.e., NO_x, CO, HC and soot were reduced by up to 18.9%, 38.8%, 71.4% and 26.3%, respectively, in $B20_{(90\ ppm)}$ compared to neat B20. The innovated fuel blend also increased engine performance parameters i.e. power and torque by up to 7.81%, 4.91%, respectively, and decreased fuel consumption by 4.50%.

Acknowledgment

The authors would like to thank Biofuel Research Team (BRTeam) for financially supporting this study.

References

[1] Hasheminejad M, Tabatabaei M, Mansourpanah Y, Javani A. Upstream and downstream strategies to economize biodiesel production. Bioresour Technol 2011;102:461–8.
[2] Choi SH, Oh Y. The emission effects by the use of biodiesel fuel. Intl J of Mod Phys B 2006;20(25–27):4481–6.
[3] Gerhard Knothe. Biodiesel and renewable diesel: a comparison. Prog Energy Combust Sci 2010;36(3):364–73.
[4] Mohadesi M, Hojabri Z, Moradi Gh. Biodiesel production using alkali earth metal oxides catalysts synthesized by sol–gel method. Biofuel Res J 2014;1:33–6.
[5] Shirazi MJA, Bazgir S, Shirazi MMA. Edible oil mill effluent; a low-cost source for economizing biodiesel production: electrospun nanofibrous coalescing filtration approach. Biofuel Res J 2014;1:39–42.
[6] Sundaramurthy J, Li N, Kumar PS, Ramakrishna S. Perspective of electrospun nanofibers in energy and environment. Biofuel Res J 2014;2:44–54.
[7] Xue J, Grift TE, Hansen AC. Effect of biodiesel on engine performances and emissions. Renew Sustain Energy Rev 2011;15:1098–116.
[8] Demirbas Ayhan. Political, economic and environmental impacts of biofuels, a review. Appl Energy 2009;86:108–17.
[9] Ameer Basha S, Raja Gopal K, Jebaraj S. A review on biodiesel production, combustion, emissions and performance. Renew Sustain Energy Rev 2009;13:1628–34.
[10] Sohpal VK, Singh A. Optimization of alkali catalyst for transesterification of jatropha cursus using adaptive neuro-fuzzy modeling. Biofuel Res J 2014;1(2):70–6.
[11] Szybist JP, Song J, Alam M, Boehman AL. Biodiesel combustion, emissions and emission control. Fuel Process Technol 2007;88:679–91.
[12] Cherng-Yuan Lin, Li Rong-Ji. Engine performance and emission characteristics of marine fish-oil biodiesel produced from the discarded parts of marine fish. Fuel Process Technol 2009;90:883–8.
[13] McCarthy P, Rasul MG, Moazzem S. Analysis and comparison of performance and emissions of an internal combustion engine fuelled with petroleum diesel and different bio-diesels. Fuel 2011;90:2147–57.
[14] Ekrem Buyukkaya. Effects of biodiesel on a DI diesel engine performance, emission and combustion characteristics. Fuel 2010;89:3099–105.
[15] Mohammadi P, Nikbakht AM, Tabatabaei M, Farhadi K, Mohebbi A. Experimental investigation of performance and emission characteristics of DI diesel engine fueled with polymer waste dissolved in biodiesel-blended diesel fuel. Energy 2012;46:596–605.
[16] Boutonnet M, Kizzling J, Stenius P. The preparation of monodisperse colloidal metal particles from microemulsions. Colloids Surf 1982;5:209–25.
[17] Zhou. Organically complexed nano-catalysts for improving combustion properties of fuels and fuel compositions incorporating such catalyst. United States Patent, US20060175230 A1, issued Aug. 10; 2006.
[18] Guru M, Karakaya U, Altiparmak D, Alicilar A. Improvement of diesel fuel properties by using additives. Energy Convers Manage 2002;43:1021–5.
[19] Chlopek Z, Darkowski A, Piaseczny L. The influence of metallo-organic fuel additives on CI engine emission. Pol J Environ Stud 2005;14:559–67.
[20] Sadhik Basha J, Anand RB. Effects of nanoparticle additive in the water-diesel emulsion fuel on the performance, emission and combustion characteristics of a diesel engine. Int J Global Warm 2010;2(4):34.
[21] Sadhik Basha J, Anand RB. The influence of nano additive blended biodiesel fuels on the working characteristics of a diesel engine. J Braz Soc Mech Sci Eng 2013;35:257–64.
[22] Calvin Hong Li. Experimental study of nanoadditives for biofuel combustion improvement. In: Proceedings of the ASME 2011 international mechanical engineering congress & exposition. IMECE2011, November 11–17, Denver (Colorado, USA); 2011.
[23] Tewari P, Doijode E, Banapurmath NR, Yaliwa VS. Experimental investigations on a diesel engine fuelled with multi-walled carbon nanotubes blended biodiesel fuels. Int J Energy Technol Adv Eng 2013;3:72–6.
[24] Rongguang L, Xiaoli LI, Qifei J. Development of high efficiency diesel fuel additive for emission control. J Vehicle Eng 2001;1:29–32.
[25] Kung HH, Kung MC. Nanotechnology: applications and potentials for heterogeneous catalysis. Catal Today 2004;97:219–24.
[26] Sadhik Basha J, Anand RB. Performance and emission characteristics of a DI compression ignition engine using carbon nanotubes blended diesel. In Proceedings of the international conference on advances in mechanical engineering. Surat, India, 3–5 August, 2009. p. 312–16.
[27] Kung HH, Kung MC. Nanotechnology: applications and potentials for heterogeneous catalysis. Catal Today 2004;97:219–24.
[28] Mills JC, Dallas TX. Fuel additive and method for use for combustion enhancement and emission reduction. United States Patent, US 8,163,044, issued Apr. 24, 2012.
[29] Tock RW, Hernandez A, Sanders JK, Yang DJ. Catalyst component for aviation and jet fuels, United States Patent, US 8,545,577, issued October 1, 2013.
[30] Sajith V, Sobhan CB, Peterson GP. Experimental investigations on the effects of cerium oxide nanoparticle fuel additives on biodiesel. Adv Mech Eng 2010. Article ID 581407.
[31] Arul Mozhi Selvan V, Anand RB, Udayakumar M. Effects of cerium oxide nanoparticle addition in diesel and diesel biodiesel-ethanol blends on the performance and emission characteristics of a CI engine. ARPN J Eng Appl Sci 2009;4:1–7.

[32] Boutonnet M, Lögdberg S, Svensson EE. Recent developments in the application of nanoparticles prepared from w/o microemulsions in heterogeneous catalysis. Curr Opin Colloid Interface Sci 2008;13:195–314.
[33] Wickham David T, Cook Ron, De Voss Sarah, Engel Jeffrey R, Nabity James. Soluble nano-catalyst for high performance flues. J Russ Laser Res 2006;27:258–68.
[34] Wang Jianwei, Liu Yang, Zhang Xiangwen, Mi Zhentao, Wang Li. Facile preparation of hydrocarbon fuel-soluble nano-catalyst and its novel application in catalytic combustion of JP-10. Catal Commun 2009;10:1518–22.
[35] Miyamoto N, Zhixin H, Harada A, Ogawa H, Murayama T. Characteristics of diesel soot suppression with soluble fuel additives. SAE technical paper No. 871612; 1987. p. 1–7.
[36] Naraghi M. Carbon nanotubes-growth and applications. Rijeka: InTech; 2011.
[37] Liu Luqi, Zhang Shuang, Tengjiao Hu, Guo Zhi-Xin. Solubilized multi-walled carbon nanotubes with broadband optical limiting effect. Chem Phys Lett 2002;359:191–5.
[38] Haddon RC, Chen J. Solubilizing single-walled carbon nanotubes by reaction with amines and alkylaryl amines. United States Patent 6187823B1; 2001.
[39] Haddon RC, Hamon MA. Method of solubilized carbon nanotubes in organic solutions. United States Patent 20010016608 A1; 2003.
[40] Feng X, Matranga C, vidic R, Borguet E. A vibrational spectroscopic study of the fate of oxygen-containing functional groups and trapped CO_2 in single-walled carbon nanotubes during thermal treatment. J Phys Chem 2004;108:19949.
[41] Ramanthan T, Fisher FT, Ruoff RS, Brinson LC. Amino-functionalized carbon nanotubes for binding to polymers and biological systems. Chem Mater 2005;17:1290–5.
[42] Sara Safari Kish, Alimorad Rashidi, Hamid Reza Aghabozorg, Leila Moradi. Increasing the octane number of gasoline using functionalized carbon nanotubes. Appl Surf Sci 2010;256:3472–7.
[43] Mohammadi P, Nikbakht AM, Tabatabae M, Farhadi Kh. A novel diesel fuel additive to improve fuel properties and to reduce emissions. Int J Automot Eng 2012;2(3).
[44] Mohammadi P, Tabatabae M, Nikbakht AM, Esmaeili Z. Improvement of the cold flow characteristics of biodiesel containing dissolved polymer wastes using acetone. Biofuel Res J 2014;2:26–9.
[45] Lam MK, Lee KT, Mohamed AR. Homogeneous, heterogeneous and enzymatic catalysis for transesterification of high free fatty acid oil (waste cooking oil) to biodiesel: a review. Biotechnol Adv 2010;28:500–18.
[46] Reed K. Cerium oxide nanoparticle-containing fuel additive, United States Patent, US 2010/0199547 A1, issued October 1, 2013.
[47] Scattergood R. Cerium oxide nano particles as fuel additives, United States Patent; US 2006/0254130 A1, issued November 16, 2006.
[48] Moy D, Niu C, Tennent H, Hoch R. Carbon nanotubes in fuels, United States Patent, US 6419717 B2, issued Jul. 16, 2002.